Check for updates

Efficient Removal of Lead and Chromium From Aqueous Media Using Selenium Based Nanocomposite Supported by Orange Peel

Maria Aziz[1], Rukhsanda Aziz[1]*, Muhammad Tariq Rafiq[2], Maryam Abbasi[1], Mehwish Taneez[3], Muhammad Usman Azhar[4], Ahmad El Askary[5], Basem H. Elesawy[6], Emad M. Eed[5], Amany S. Khalifa[7] and Abdul Qayyum[8]*

[1]Department of Environmental Science, International Islamic University, Islamabad, Pakistan, [2]Centre for Interdisciplinary Research in Basic Sciences, International Islamic University, Islamabad, Pakistan, [3]Department of Civil, Environmental and Natural Resources Engineering, Luleå University of Technology, Luleå, Sweden, [4]Department of Earth Sciences, The University of Haripur, Haripur, Pakistan, [5]Department of Clinical Laboratory Sciences, College of Applied Medical Sciences, Taif University, Taif, Saudi Arabia, [6]Department of Pathology, College of Medicine, Taif University, Taif, Saudi Arabia, [7]Department of Clinical Pathology and Pharmaceutics, College of Pharmacy, Taif University, Taif, Saudi Arabia, [8]Department of Agronomy, The University of Haripur, Haripur , Pakistan

This study presents the synthesis of activated orange peel, derived from bio-waste (orange peel) and its doping with selenium nano-particles to enhance the adsorption capacity. The synthesized nanocomposite orange peel/Selenium (OP/Se) was applied as adsorbents for the removal of Lead (Pb) and Chromium (Cr) from synthetic waste water as an economical water cleaning technology. Orange peel/Selenium nanocomposite was characterized by X-Ray diffraction (XRD), Fourier transform infrared spectroscopy (FT-IR) and Scanning electron microscopy (SEM). Scanning electron microscopy results showed the porous structure of OP/Se nanocomposite and distinct peaks observed in XRD and FTIR spectra depicted the successful synthesis of nanocomposite. Batch experiments were conducted to figure out the effect of different parameters on adsorption of Pb and Cr by using Atomic Absorption Spectroscopy. The maximum adsorption capacity of 99.9% was achieved for both lead and chromium at acidic pH. While at temperature of 60°C the maximum adsorption of 98.3 and 95.9% was found for Pb and Cr respectively. Furthermore the experimental data was examined with Pseudo-first order, first-order and Pseudo-second order kinetic model, as well as Morris Intraparticle diffusion model where the pseudo second order was best fitted which indicated the chemisorption mechanism in adsorption process. The adsorption process followed the Langmuir isotherm model verified that OP/Se nanocomposite was found to be favorable for the process of adsorption. The adsorption thermodynamics indicate that adsorption of heavy metals ions is spontaneous ($\Delta G° < 0$) and the adsorption increases with increase in temperature which means that reaction was endothermic in nature. This study revealed that the synthesized bio-activated nanocomposite was an efficient adsorbent material for the removal of heavy metals from waste water.

1 INTRODUCTION

Heavy metals are the most hazardous contaminants among all the pollutants found in water and are of major concern because they are non-biodegradable in nature having serious effects on both human and environmental health. Excessive release of heavy metals into the environment has posed a great threat worldwide due to their non-biodegradable and toxic nature even at low concentrations (Gupta et al., 2011). They are introduced naturally (weathering) as well as through anthropogenic activities which include mining, electroplating, smelting, and industrial processes (Nriagu, 1996; Akbar et al., 2006). This situation affects ground and surface water with a number of health problems. Lead can affect nervous system, inhibit enzyme activities and formation of red blood cells even at low concentration (Igwe and Abia, 2007). Several countries release effluents without any prior treatment to surface water (Srivastava and Banik, 2003), making it crucial to remove the hazardous pollutants (Khan et al., 2012).

Treatment technologies for both drinking water and wastewater are one of the most important key concerns for sustaining human well-being. The use of polymer-based synthetic fibres composites started in many applications in 1930 on account of their high specific stiffness and strength (Begum and Islam, 2013; Jagadeesh et al., 2017; Keya et al., 2019). However, the use of synthetic fibres in polymer composites is fading every day for the sake of its excessive processing cost, nonbiodegradability, and non-skin-friendliness behaviour (Mohammed et al., 2015; Sahu and Gupta, 2019; Thyavihalli Girijappa et al., 2019; Sahu and Gupta, 2020). Furthermore, the numerous uses of nonbiodegradable polymer-based synthetic fibres in many engineering applications led to environmental imbalance. Therefore, the development of an eco-friendly and sustainable composite material (i.e., biocomposites) is needed to protect our environment. In this context, the researchers have successfully tried to replace these nonbiodegradable and non-eco-friendly synthetic fibres with natural fibres which can replace these synthetic fibres in many cases.

The traditional waste water treatment technologies have insufficient potential for acceptable elimination of pathogenic microorganisms and a widespread range of hazardous substances and pollutants in wastewater. Cost is an important parameter for comparing the sorbent materials. However the expense of individual sorbents varies depending on the degree of processing required and local availability. Therefore, it is pivotal to introduce advanced water treatment technologies with low energy consumption and higher efficiencies (Libert et al., 2007). In this perspective, different conventional technologies including adsorption (Davarnejad and Panahi, 2016), membrane filtration (Landaburu-Aguirre et al., 2010), solvent extraction (Lertlapwasin et al., 2010), electrochemical treatment (Akbal and Camcı, 2011), chemical precipitation (Fu and Wang, 2011) and ion exchange (Verma and Singh, 2008; Lai et al., 2016) have been used for the removal of heavy metals. But

all these technologies are associated with complicated procedure and are too costly to maintain, generally producing toxic sludge (Bhatnagar et al., 2015). Therefore, among all these technologies, adsorption is the most appropriate technology due to its high competence as well as profitable consideration (Gupta et al., 2016). Adsorption is the adhesion of molecules or ions onto solid surface has been documented as efficient method for the removal heavy metals from contaminated water as it is cheap and eco-friendly (Lau et al., 2007; Gavrilescu, 2014).
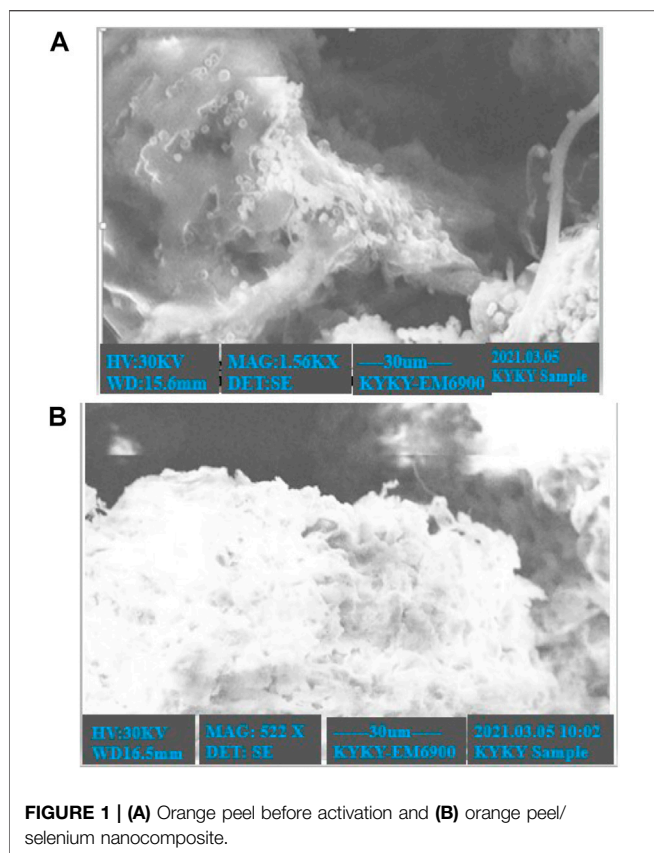
As the agricultural wastes are available in sufficient quantities in agricultural countries it make possible to use them as a natural adsorbents. They can be effectively used to develop a value-added product with enhanced performance properties (Shaker et al., 2020). Mechanical properties of composite reinforced with fibers enhances strength at the micro level, to reduce cracks and to make it lighter in weight (Ugbolue et al., 2011; Zeeshan et al., 2021).

Agronomic materials include a variety of functional groups, lignin, lipids proteins, hydrocarbons and starch. Adsorbents such as zeolites, activated carbon, polymers, and biomaterials are using on large scale for the treatment of wastewater (Weber and Morris, 1963).

A number of adsorbents including olive cake (Doyurum and Çelik, 2006), bone meal-derived apatite (Yobas et al., 2009), fish scale (Ofudje et al., 2018), tea-industry waste (Cay et al., 2004), orange peel (Biccard et al., 2018), banana peel (Updyke et al., 2012), pomegranate (Jaouali et al., 2018) and corn cob (Buasri et al., 2012) have been reported for their capability to eliminate heavy metals from waste water because they include a variety of functional groups. The use of these waste agricultural by-products has gain great momentum recently as they are simple, freely available, require low cost of production and do not generate secondary pollutants. Ajmal et al. (Ajmal et al., 2000), has used orange peel adsorbent for the removal of nickel. Another study was conducted on the removal of Cr (VI) from wastewater by using rice husk adsorbent (Hong et al., 2003). Pecan shell has been used as an adsorbent for the removal of Zn(II) and Cr(II) from wastewater (Bansode et al., 2003).

Orange peels have been recognized and accepted as an agro-industrial residue from literature, with adsorptive efficiencies and have been used in adsorption process (Anhwange et al., 2009; Rani and Ravindhranath, 2014). It is essentially composed of cellulose, hemi-celluloses, pectin, chlorophyll pigments, lignin and number of other low molecular weight compounds. The orange peels act as a polymer material in the adsorption process which is highly used in the wastewater treatment as adsorbents, because they have high surface areas and active functional groups involved such as oxygen. These functional groups are categorized into acidic or basic which affect the surface charge and ultimately enhance its biosorption capacity (Ayatollahi et al., 2013; Rajoriya and Kaur, 2014).

In contrast to traditional materials, the adsorbents doped with nano-particles show greater adsorption rates and higher competence for the treatment of wastewater (Asfaram et al., 2017). Nano scale iron supported by corn cob and silver oxide/

FIGURE 1 | **(A)** Orange peel before activation and **(B)** orange peel/selenium nanocomposite.

FIGURE 2 | FT-IR spectra of orange peel and orange peel/selenium nanocomposite.

sawdust nanocomposite has been used for the removal of hexavalent chromium from aqueous media (Dobaradaran et al., 2017; Kumari et al., 2018). Another study has reported the removal of copper from contaminated water with sugarcane bagasse derived nano-magnetic adsorbent (Wannahari et al., 2018). Selenium nanoparticles have a high specific surface area and number of different surface active centers which are useful for better adsorption capacities (Belal et al., 2014). In an another study selenium nanoparticles have been used for the adsorption of Hg from fluorescent lamp vapors (Brandstätter et al., 2008) as well as Zn and Cu from synthetic wastewater (Zhang et al., 2011; Le Quéré et al., 2015). Selenium is an essential element because it is important for the process of metabolism. For example, up to 40 µg/day of dietary selenium is essential for human health. Several studies revealed that elemental Se at nano size (Nano-Se) is less toxic as compared to selenite (Zhang et al., 2005; Wang et al., 2007). Nano-Se can serve as an antioxidant with reduced risk of Se toxicity and a potential chemo preventive agent. Another study has reported that nano-Se is a potential selenium source with a prominent characteristic of lower toxicity (Bathe and Zhang, 2004). Because of its semiconducting and photoelectric nature, anti-cancer, free radical scavenging ability and anti-oxidative properties, Se has attracted great attention (Lenz et al., 2008).

This present study deals with the assessment of efficiency and effectiveness of Orange peel and Selenium nanocomposite (OP/
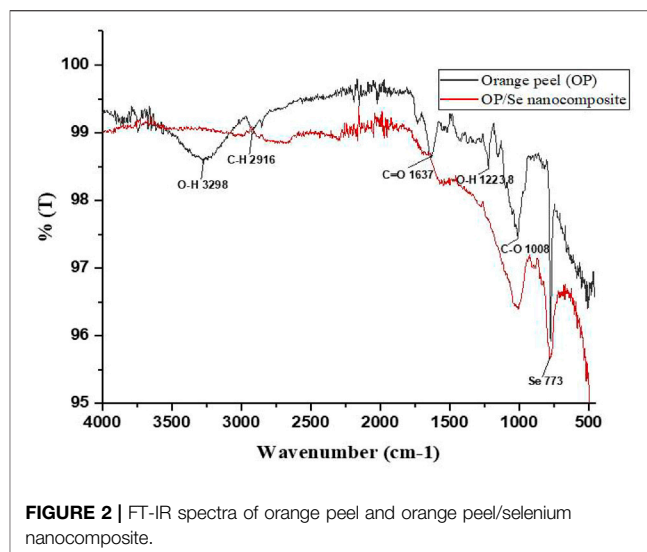
Se). Previous studies have not reported the doping of Orange peel as polymer adsorbent with nano-selenium. Therefore, this study focuses on the synthesis of Orange peel/selenium nanocomposite for the removal of heavy metals Lead (Pb) and Chromium (Cr) on a lab scale. Selenium nanoparticles are made as a by-product of the microbial conversion of selenium oxyanions in bioreactors (Sharma et al., 2014) as well in environment (Jain et al., 2016) which provide very easy and efficient solid–liquid separation through simple gravity settling after adsorption of heavy metals (Zheng et al., 2019).

2 MATERIALS AND METHODS

2.1 Synthesis of Activated Orange Peel
Orange peels (OP) samples were collected from local market of Islamabad, Pakistan cut down into pieces, and washed two to three times by using tap water to remove extraneous materials (dirt and sands). After washing these sample materials were dried in the presence of sunlight for 1 week. The dried orange peel samples were crushed to a powder form with the help of grinder. Furthermore, it is subjected to NaOH activation in the ratio of 10:8 (weight/g) OP and NaOH respectively at 100°C/200 rpm for 7 h. It was washed by de-ionized water to get neutral pH and treated with Hydrochloric acid (2M) under water bath at 80°C for 25–30 min to remove residual alkali metals in samples. At the end this prepared activated orange peel sample was washed again by using de-ionized water till it became colorless and neutral. Finally, it was dried at 80°C for 4 h (Finkelstein et al., 2014).

2.2 Synthesis of Selenium Nanoparticles
Selenium nanoparticles (SeNPs) were prepared by chemical precipitation/reduction method. Sodium selenite (Na_2SeO_3) and ascorbic acid ($C_6H_8O_6$) were used for the preparation of nanoparticles of Selenium where ascorbic acid ($C_6H_8O_6$) acts as a reducing operator (Bahig and El-Kadi, 2016). Aqueous solution
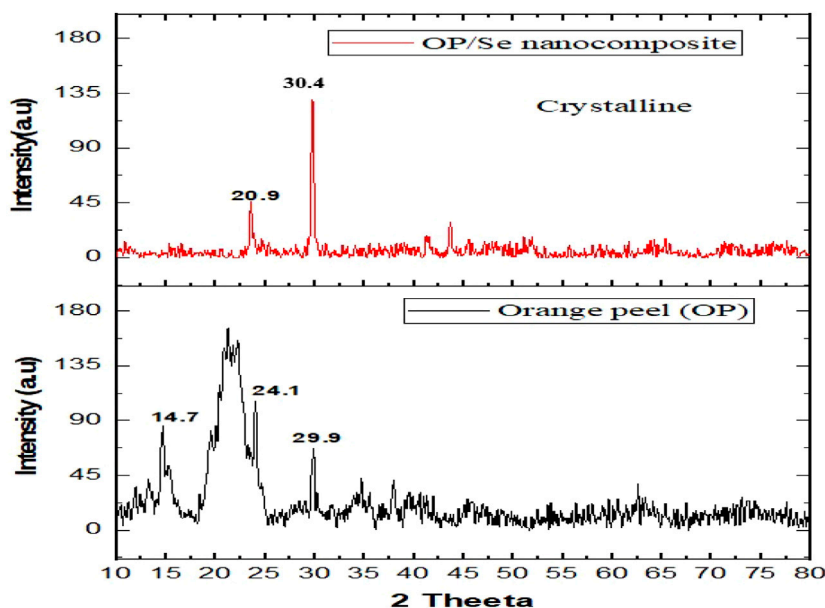
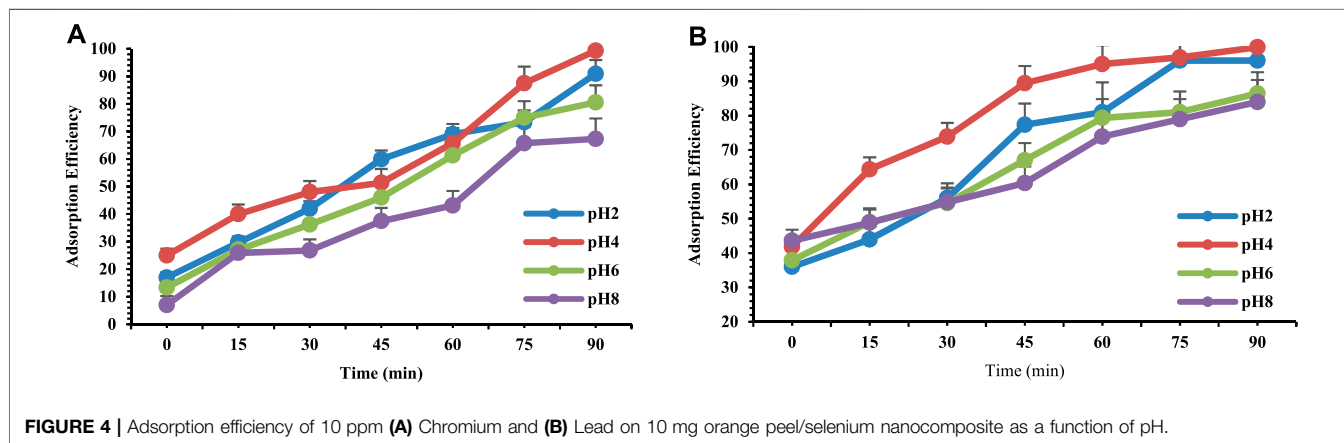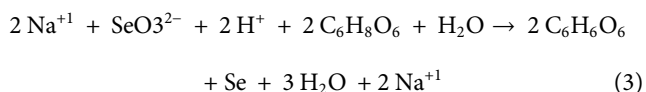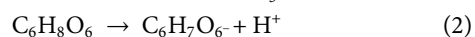**FIGURE 3 |** XRD spectra of orange peel and orange peel/selenium nanocomposite.

FIGURE 4 | Adsorption efficiency of 10 ppm **(A)** Chromium and **(B)** Lead on 10 mg orange peel/selenium nanocomposite as a function of pH.

of 17.29 g Na_2SeO_3 and 8.806 g $C_6H_8O_6$ were prepared in a ratio of 1:4. After that solution was kept under magnetic stirring at ambient temperature for 30 min. Mixtures were allowed to react with each other in the concentrated form until the color of solution change from colorless to red color where ascorbic acid has reduced the composition of sodium selenite during the reaction (leaving Se particles in the solution) and resulted in red nano-selenium. Finally, when red color appeared then the solution was centrifuged at 3,000 rpm and the Selenium nanoparticles were obtained and dried at $40^{\circ}C$.

$$Na_2SeO_3 \rightarrow 2\,Na^+ + SeO_3^{2-} \tag{1}$$

$$C_6H_8O_6 \rightarrow C_6H_7O_{6^-} + H^+ \tag{2}$$

$$2\,Na^{+1} + SeO3^{2-} + 2\,H^+ + 2\,C_6H_8O_6 + H_2O \rightarrow 2\,C_6H_6O_6$$
$$+ Se + 3\,H_2O + 2\,Na^{+1} \tag{3}$$

2.3 Preparation of Orange Peel/Selenium (OP/Se) Nanocomposite

3 g of activated orange peel was mixed with 7 g of Se nanoparticles, and then mixture was added in 30 ml of distilled water and agitated for half an hour with the help of magnetic stirrer. After that it was shifted to a 50 ml vessel and heated on hot plate with magnetic stirring at $200^{\circ}C$ for 24 h, then resulted sample was washed two times using both ethanol and distilled water and dried at $60^{\circ}C$ then calcined at $550^{\circ}C$ in muffle furnace for 3 h. The obtained product was expressed as OP/Se nanocomposite and placed in a desiccator for further use in experiment.

2.4 Characterization Studies

Characterization studies of sample have been performed through using SEM, XRD and FT-IR. Scanning electron microscopy of

FIGURE 5 | Adsorption efficiency of 10 ppm **(A)** Chromium and **(B)** Lead at pH 4 on orange peel/selenium nanocomposite as a function of adsorbent dose.
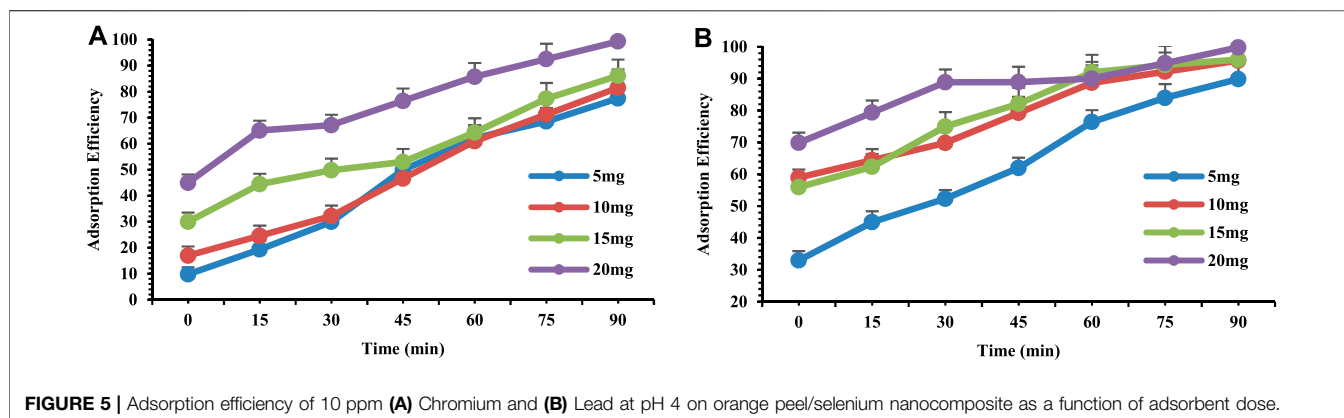
samples was carried out at different magnifications in order to study the surface morphology of sample under characterization through using KYKEM6900 (Eindhoven, Netherlands) at the voltage of 30 KV, current 2.7 A, and distance of 10–15 nm. The XRD was carried out through using D8 Advance by Bruker Germany X-ray powder diffraction microscopy (time step 0.1 s, increment 0.02, 2 theta from 10 to 70 nm, voltage 40 KV and current 30 mA) while in order to determine the functional groups on the adsorbent FT-IR (PerkinElmer, Waltham, MA, United States) was performed at an infrared range of 4,000 and 500 cm^{-1} as wave numbers.

2.5 Batch Adsorption Experiment

The OP/Se nanocomposite was applied as bio-sorbent for the treatment of selected heavy metals (Pb and Cr) by preparing the stock solutions of lead (Pb) and potassium chromate (K_2CrO_4) in 100 ml distilled water. Working solutions having concentration of 10 and 20 ppm were prepared through dilution of both of the standard solutions (stock). Series of batch experiment were conducted under variable parameters of pH (2, 4, 6, 8), temperature (30°C, 40°C, 50°C, 60°C), initial metal ion concentration (5, 10, 15, 20 ppm) and dose of adsorbent (5, 10, 15, 20 mg) at a shaking speed of 100 rpm (HY-4A CYCLING) and contact time of 90 min. Samples were collected after interval of every15 min and labelled. Each solution pH was settled by using of 1M HCl or 1M NaOH solution. At the end each filtrate was run on Atomic Adsorption Spectrophotometer (AA-7000, SHIMADZU) for examining the quantity of metals adsorbed at conditions for quantification including standard 1,3; 5 ppm solution from 1,000 ppm stock solution; burner height of 7 cm and gas air acetylene has been used at 0.9 PSI pressure and the wavelength between 190 and about 320 nm.

2.6 Adsorption Kinetics

The kinetic models have been applied to fit the experimental data in order to examine the mechanism of adsorption, which controls the process of adsorption. In this research study experimental data was examined with Pseudo-first order, first-order and Pseudo-second order kinetic model, as well as Morris Intraparticle diffusion model.
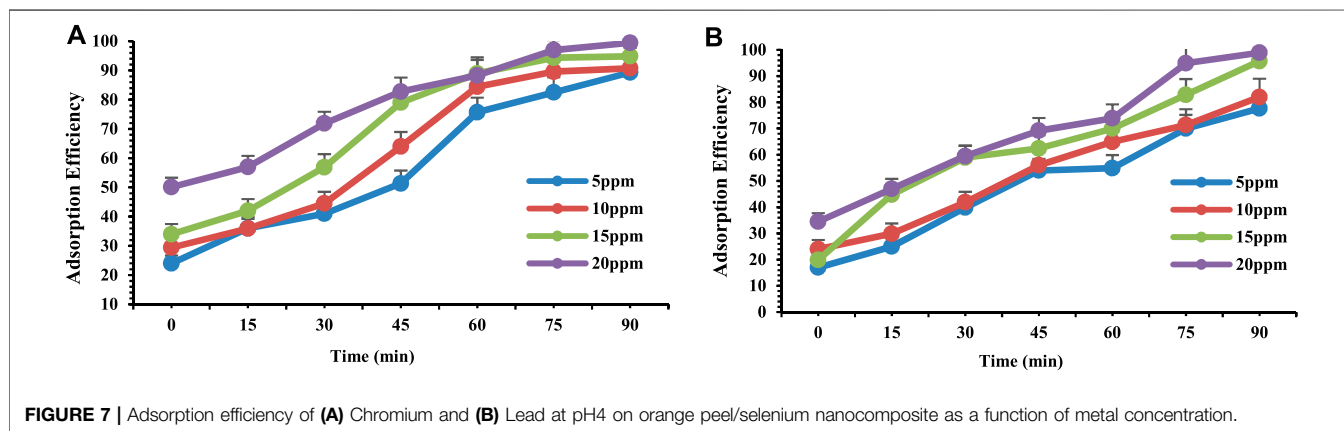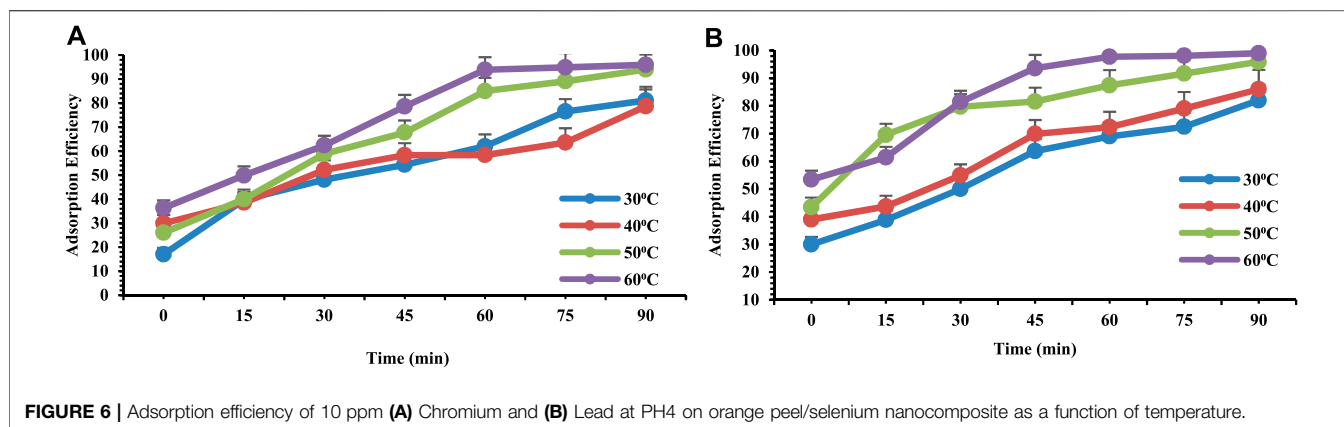
3 RESULTS

3.1 Characterization of Adsorbent

Scanning electron microscopy (SEM) was used to observe the structural morphology of synthesized adsorbents. It was observed that there is no pore formation and orange peel (OP) has smooth surface before activation (**Figure 1A**. In **Figure 1B** pore structure of OP/Se nanocomposite was observed which act as active sites where adsorption takes place. It was also found that it contains irregular intercellular spacing and pores which are formed due to the NaOH activation. Concerning with structural morphology pores formation is a strong evidence for adsorbent to adsorb heavy metals from aqueous solution because the pores present on the surface enhance the contact area during adsorption (Chukwuemeka-Okorie et al., 2018). Another study reported that an internal surface and pores are necessary for an efficient biosorption process (Mangal et al., 2015).

FT-IR spectra were captured in the frequency range from 400 to 4,000 cm^{-1} which helps to identify elements involved in structural modification. FTIR spectrum of OP (**Figure 2**) represents the peak at 3,298 cm^{-1} indicating the stretching vibration of O-H bond in hydroxyl group. The peak at 2,916 cm^{-1} and the peak at 1,637 cm^{-1} is due to–CH and C=O stretching vibrations respectively. While the peaks at 1,223.8 cm^{-1} and 1,008 cm^{-1} are related to O-H and C-O vibrations (Androulaki et al., 2018). In contrast OP/Se nanocomposite shows more pronounced peak at 773 cm^{-1} which is due to the presence of metal (**Figure 2**). Several studies has also observed metal peak in this region which is closely supported by the reports of Mudhaffar and Hasan (Shoukry et al., 2015) where characteristic strong bands due to C=Se were observed. Moreover other peaks were found to be diminished after doping it with Selenium nanoparticles as metal has occupied the space except for C-O vibrations in OP/Se nanocomposite spectra. These results show the successful formation of OP/Se nanocomposite.

XRD was performed to examine the geometrical features of the synthesized adsorbents (**Figure 3**). XRD spectra of OP shows broad peak between 14.7° and 24.1° corresponding to phases of (110) and 200) respectively. While relatively sharp peaks were appeared in OP/Se nanocomposite after doping Se nano-particles
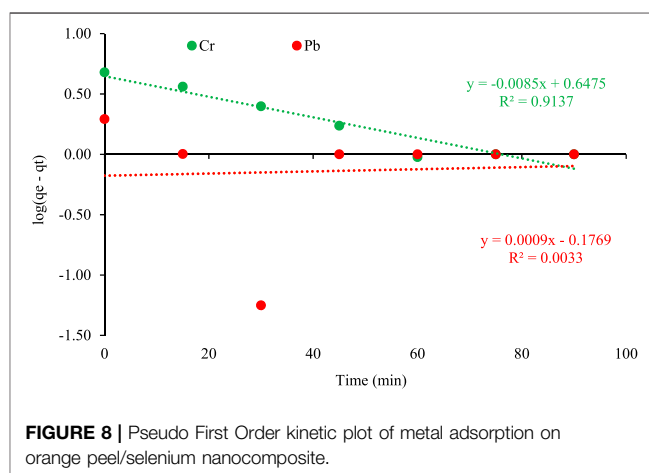
FIGURE 6 | Adsorption efficiency of 10 ppm **(A)** Chromium and **(B)** Lead at PH4 on orange peel/selenium nanocomposite as a function of temperature.

FIGURE 7 | Adsorption efficiency of **(A)** Chromium and **(B)** Lead at pH4 on orange peel/selenium nanocomposite as a function of metal concentration.

at 20.9⁰ and 30.4⁰ with respective phases of (100) and (101) in accordance with JCPDS No. 06-0362. The significant change in spectra shows the formation of nanocomposite. OP/Se nanocomposite was found to be crystalline in nature which is an important factor for the adsorption. Addition of activated orange peel results in peak shift from broad (which indicate the highly amorphous structure) to sharp which also confirm the formation of nanocomposite. The development of sharp peaks in the resulted spectrum obtained suggested good crystallinity of Se/ OP Nano-composite as according to Ghada and Bahig for effective adsorption crystalline nature of the adsorbent is an important factor (Nuhoglu and Oguz, 2003).
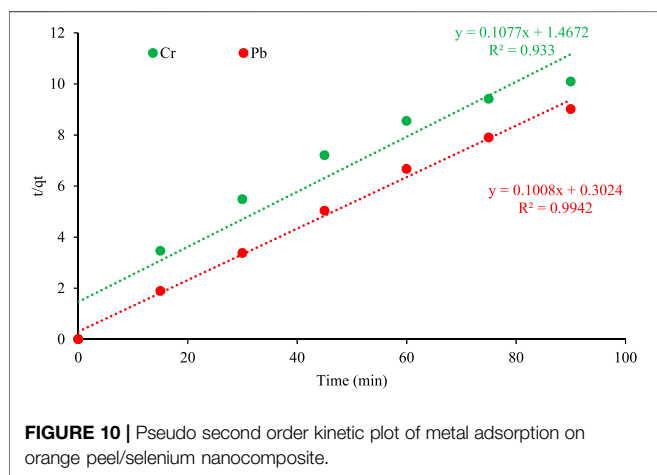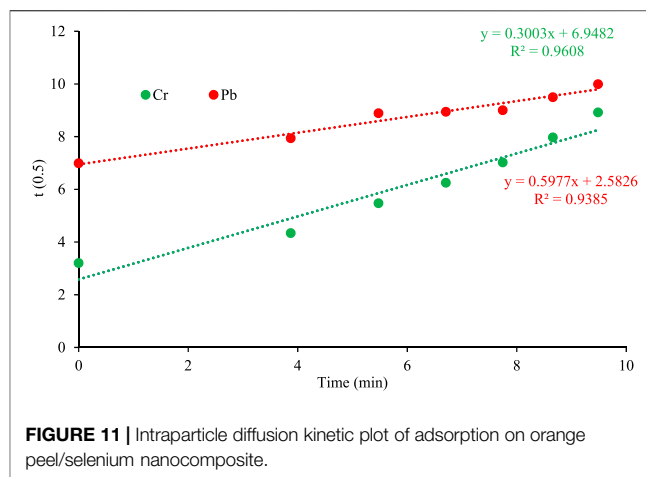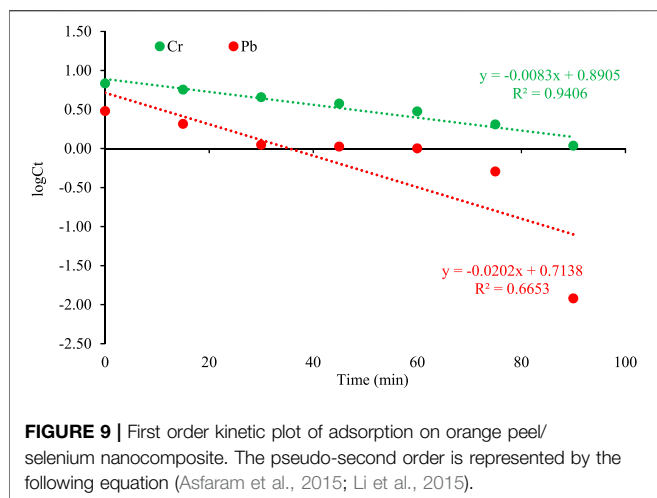
3.2 Batch Adsorption Experiments
3.2.1 Effect of Solution pH on Adsorption
The pH of waste water is a significant key controlling parameter that governs adsorption of toxic substances from wastewater (Chukwuemeka-Okorie et al., 2018). In this current study an experiment was conducted at different pH i.e. 2, 4, 6, 8 to study the influence of pH on the adsorption of selected heavy metals i.e. Lead and Chromium. **Figure 4A** represents the gradual increase in the adsorption of chromium at both acidic and basic pH. By increasing the pH up-to 8 the percentage removal also increased gradually (Lenz et al., 2008) but at pH 8.5 precipitation was observed therefore the reaction was stopped and carried out till

FIGURE 8 | Pseudo First Order kinetic plot of metal adsorption on orange peel/selenium nanocomposite.

pH 8 (Liu et al., 2013). However, at pH4 there is a constant adsorption between 60 and 75 min in case of Lead (see **Figure 4B**). The network of charges of the adsorbate and adsorbent depends on the pH of solution (Luisa et al., 2021). Maximum adsorption efficiency was found to be 99% at acidic pH for both Chromium and Lead. Therefore, acidic medium was found to be better for both Chromium and Lead adsorption. At acidic pH higher protic environment favors the adsorption.

FIGURE 9 | First order kinetic plot of adsorption on orange peel/selenium nanocomposite. The pseudo-second order is represented by the following equation (Asfaram et al., 2015; Li et al., 2015).

FIGURE 11 | Intraparticle diffusion kinetic plot of adsorption on orange peel/selenium nanocomposite.
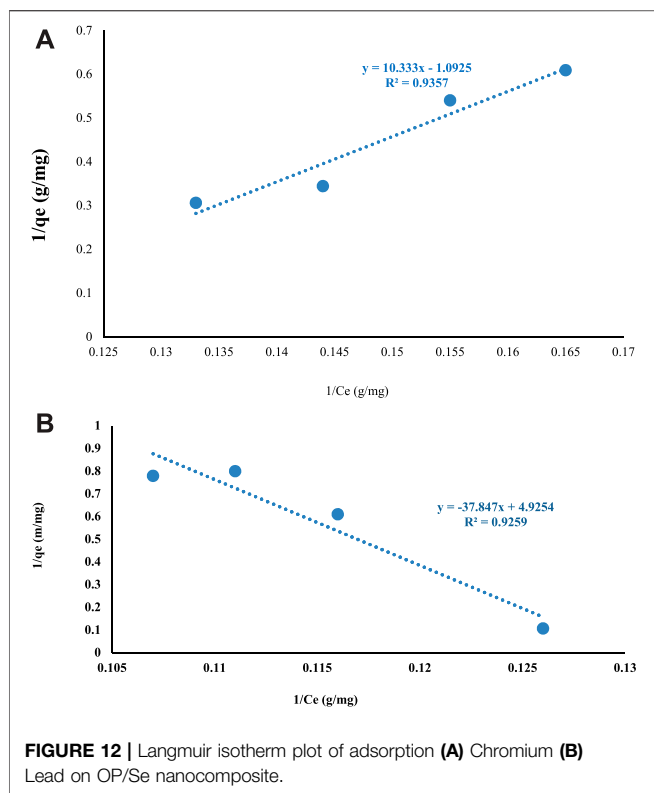
3.2.2 Effect of Adsorbent Dose

Adsorbent dosage is a key important factor for controlling the availability and accessibility of adsorption sites (Dehghani et al., 2016). In the current study in order to examine the effect and consequence of adsorbent dose, varying doses of adsorbent (5 mg, 10 mg, 15 mg and 20 mg) were used for both Pb and Cr. According to the results shown in **Figure 5A,B** it is evident that as the adsorbent dose increased the adsorption of metals also increased. This is for the reason that with greater dose of sorbent, more binding sites become available and accessible for both Pb and Cr on the surface of adsorbent, which leads towards the greater removal capability. In general, greater adsorbent dose and lesser Pb and Cr ions concentration boosted and enhance the uptake (Gangadhar et al., 2016). Arica et al. (2018) observed that by increasing the adsorbent dose there is an increase in the available sites on the adsorbent for the uptake of the adsorbate which ultimately lead towards an increase in the adsorption efficiency of adsorbent (Sulyman et al., 2016).

Gangadhar et al. (Robati et al., 2016), also studied the influence of adsorbent dose for the adsorption of both Malathion and Phorate which showed that adsorption capacity was increased as the amount of adsorbent increased. Increased adsorbent dose will definitely enhance the number of active sites for adsorption and ultimately increase the adsorbent surface area (Jiang et al., 2018).

Therefore, with the support of literature it can be concluded that OP/Se Nano-composite has a unique adsorption capacity because of maximum removal of 99% at the dose of 20 mg (**Figure 5A,B**).

3.2.3 Effect of Temperature

The temperature is most effective parameter for heavy metal adsorption. In this present study in order to examine and evaluate the effect of temperature on the efficiency of adsorption, varied temperature were used i.e. 30°C, 40°C, 50°C and 60°C for both Pb and Cr. The results (**Figure 6A,B**) showed that by increasing the temperature the adsorption efficiency for metals increases as well. In our present study at higher temperature (60°C), the adsorption

FIGURE 10 | Pseudo second order kinetic plot of metal adsorption on orange peel/selenium nanocomposite.

A research study observed that a decrease of removal may occur with an increase in pH level above pH 8 (Ozalp et al., 2015) because of anionic form of chromium in an aqueous solution being favorable to adsorption because it has a surface containing a large amount of H^+ ions due to the acidified pH (Bayramoglu and Arica, 2018). This behavior was verified in the adsorption with the chestnut shell, the highest adsorption was verified at pH 4.5. Similar results were presented for Trapa bispinosa's peel bio-sorbent chemically treated to enhance adsorption capacity for Pb (II) where acidic medium was best for adsorption (Nie et al., 2015). Bayramoglu and Arica observed that the decrease or increase of biosorption capacity of U (VI) at different pH medium can be recognized to the change in surface characteristics of the adsorbent (Song et al., 2013). Additionally it was examined that the surface characteristics of those adsorbents were composed of different functional groups including hydroxyl, carboxyl, carbonyl, amine, and phosphate groups where electrostatic interactions and ion-exchange are primarily responsible for the process of biosorption.

FIGURE 12 | Langmuir isotherm plot of adsorption **(A)** Chromium **(B)** Lead on OP/Se nanocomposite.

FIGURE 13 | Freundlich isotherm plot of adsorption (A) Chromium (B) Lead on OP/Se nanocomposite.

capacity of OP/Se nanocomposite increased for both Pb and Cr, may be due to enhancement of inter-reaction between adsorbent and adsorbate leading towards formation of new adsorption sites with large surface area (Rangabhashiyam et al., 2015). There are lower intramolecular energies at higher temperature. Therefore increased temperatures promoted the efficiency of adsorption (Tan et al., 2008). An increasing number of molecules may acquire sufficient energy to undergo an interaction with active site at the surface at an elevated temperature that may increase the kinetic energy and the mobility of metal ions to be adsorbed on adsorbent surface (Akinhanmi et al., 2020).

Increase in temperature lead towards increase in the rate of the progression of both Pb and Cr ions from the solution onto the empty sites of OP and weakened the thickness of the surface layer of OP, thus ultimately enhancing the dispersion resistance of adsorbates to adsorbents (Yobas et al., 2009). Due to rise in temperature of the solution the adsorption competence of both the metals on biopolymer (OP/Se nanocomposite) increased indicating that the process was endothermic in nature.

3.2.4 Effect of Adsorbate Concentration
The effect of the concentration of adsorbate was also studied at different time intervals. According to the results (**Figure 7A,B**) it is evident that with the change in concentration of adsorbate the adsorption was increased by increasing the concentration.

In another study (Dehghani et al., 2016) examined the effect of concentration where the concentration of sorbate was varied over the range of 10–50 mg/L in the presence of 10 mg of adsorbent. In this research study it was observed that by increasing the
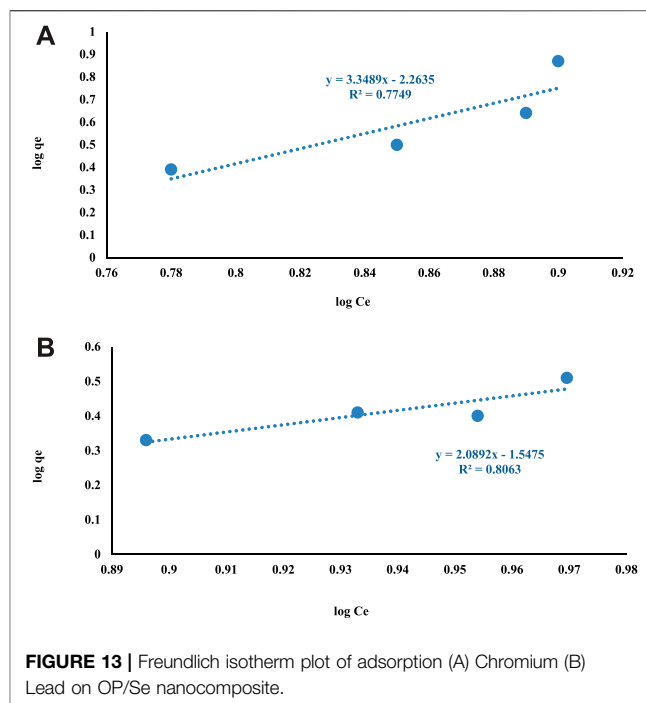
concentration of sorbate the adsorption efficiency of phenanthrene was increased (Bayramoglu and Arica, 2018). By increasing the initial concentration of both the metals in the solution, the amount of the metal ions adsorbed onto the adsorbent surface equally increased which could be a consequence of the increase in the number of the molecules of metal ions per unit volume of the solution (Nie et al., 2015).

Therefore 20 ppm adsorbent dose was found to be effective for increased concentration of metals (Cr and Pb) which reveals the efficiency of synthesized OP/Se nanocomposite.

3.3 Adsorption Kinetics
The kinetic models have been applied to fit the experimental data in order to examine the mechanism of adsorption, which controls the process of adsorption. In this research study experimental data was examined with Pseudo-first order, first-order and Pseudo-second order kinetic model, as well as Morris Intraparticle diffusion model.

In general the pseudo-first order kinetic model (Liu et al., 2013) is expressed as **Eq. 4**

$$dqt/dt = k1(qe - qt). \qquad (4)$$

k1 represents the pseudo-first order rate constant (min^{-1}), qt is the amount of solute adsorbed at time t (min) and qe is the amount of solute (mg/g) adsorbed at saturation. The integrated form of this equation is represented as following in **Eq. 5**;

$$log(qe - qt) = log qt - k1t \qquad (5)$$

Plot of log(qe − qt) verses t is shown in **Figure 8**.

The fitness of the Pseudo first order model is not applicable for Lead in comparison to Chromium. Another study reported that

FIGURE 14 | Linear fitting on the adsorption data of **(A)** chromium and **(B)** lead.
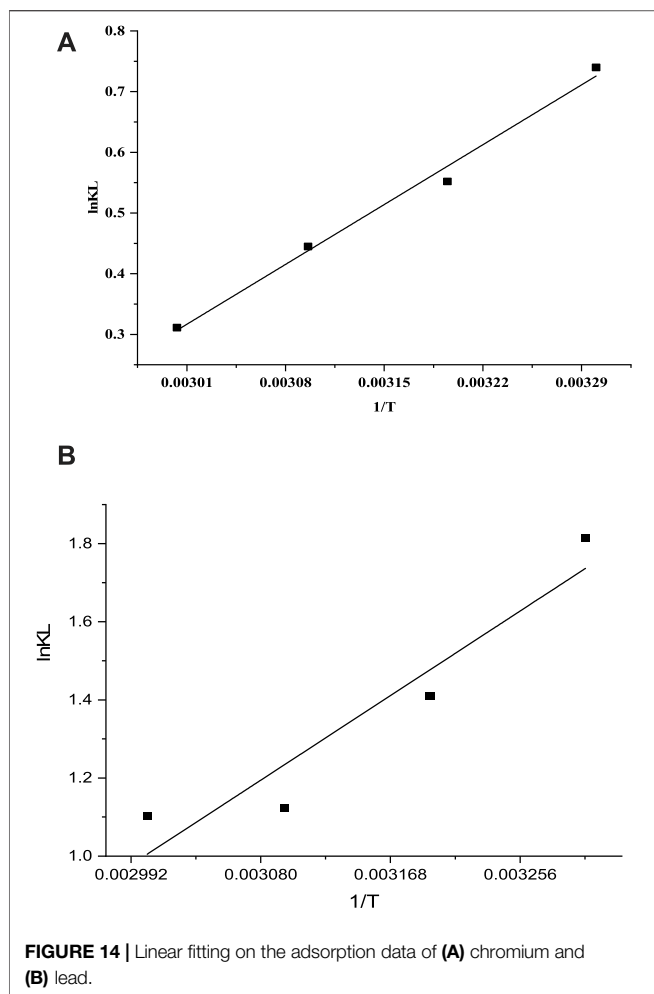
pseudo first order was found to be unfit for the adsorption of heavy metals because the values of qe (calculated) disagree with the experimental values of qe (Dongyan et al., 2016). Ofomaja et al. (Ofomaja et al., 2020), also observed similar results for the adsorption of chromium metal.

First-order reaction is a reaction that proceeds at a rate that depends linearly on the concentration of just one reactant. It is represented in following equation;

$$\log C_t = [K1\sigma/2.303]\,t + \log Co \qquad (6)$$

Figure 9 show the trends kinetic model for chromium and lead which described that the model fits with the chromium adsorption in comparison to lead.

$$t/qt = 1/k2qe^2 + t/q_e \qquad (7)$$

While k2 (min/mg) is the pseudo-second order rate constant and qe is the amount adsorbed at equilibrium (mg/g). The plot of t/qt versus t gave straight line for Chromium and Lead with R2 value of 0.93 and 0.99 respectively (**Figure 10**). The excellent agreement of experimental data to pseudo second order model postulates that adsorption follows the chemisorption mechanism. The fast and efficiency of each material is well suited to the model.

Intraparticle diffusion model was proposed by Weber and Morris (Weber and Morris, 1963) and it is represented by the following eq;

$$qt = kpt^{1/2} + C \qquad (8)$$

Where kp represent the Intraparticle diffusion rate constant (mg/g min1/2) and intercept of plot C represents surface adsorption. **Figure 11** demonstrates the diffusion model for Chromium and Lead where the value of intercept is greater for both metals depicting the greater contribution of surface adsorption in the rate-limiting step. The plot of qt versus t1/2 does not pass through the origin therefore, Intraparticle diffusion is not only the rate limiting step but also the external mass transfer plays an important role in the adsorption process (Al-Ghouti et al., 2009; Kumar and Gaur, 2011).

3.4 Adsorption Isotherms

Two adsorption isotherm models i.e. Langmuir and Freundlich were applied to fit the experimental data in order to examine the relationship between the adsorbate and adsorbent concentrations at equilibrium.

The Langmuir isotherm is generally applied to model monolayer adsorption on homogeneous and energetically uniform surfaces which can be expressed in the form of **Eq. 5**, (Tee et al., 2009).

$$1/qe = (1/Ka\,qm)1/Ce + 1/qm \qquad (5a)$$

In **Equation 5** Ka (L mg−1) represents the Langmuir equilibrium adsorption constant i.e. the energy of sorption and q_m (mg g−1) is the Langmuir maximum sorption capacity. A

TABLE 1 | Thermodynamic parameters for chromium and lead adsorption.

	Temp (K)	KL	ΔH^0 KJmol^{-1}	ΔHJK^{-1}mol^{-1}	ΔH JK^{-1}mol^{-1}	R2
Chromium	303	2.095	−1.863	11.721	32.649	0.985
	313	1.736	−1.436			
	323	1.561	−1.194			
	333	1.365	−0.861			
Lead	303	6.131	−4.568	20.459	53.085	0.853
	313	4.100	−3.672			
	323	3.075	−3.017			
	333	3.016	−3.056			

linear plot of $1/q_e$ against $1/C_e$ was plotted (**Figure 12A,B**). The values of q_m and K_a were calculated from the slope and intercept of the graph. The dimensionless constant RL was calculated through the following Eq.

$$RL = 1/1 + Ka\,C0 \dotsfill K\,)$$

Where C_0 represent the initial concentration while K_a represent the Langmuir constant. The value of RL is used to find out whether the adsorption is favorable or not for Langmuir type of adsorption. RL < 1 indicate the favorable adsorption while RL > 1 constitutes an unfavorable adsorption.

The Freundlich isotherm model is applied in order to determine adsorption intensity of adsorbate surfaces with non-uniform energy distribution. The linear form of Freundlich equation can be written as;

$$Log\ qe = log\ K_F + 1/n\ log\ Ce \qquad (7a)$$

In the above equation n represents the Freundlich constant which is related to the intensity of adsorption while K_F (L mg^{-1}) is the Freundlich adsorption constant related to the adsorption capacity. A plot of $log\ q_e$ against $log\ C_e$ was plotted which gives a straight line. **Figure 13A,B** and **Figure 14A,B** represents that the Langmuir adsorption isotherm is well fitted for both Pb and Cr as compared to Freundlich isotherm model (Mehmoud and Halwany, 2014) because it yield a higher correlation coefficient value than Freundlich isotherm model (Al-Mudhaffar and Hasan, 2012). Another study reported that Langmuir isotherm models was applicable for the removal of heavy metals by using Orange peel as an adsorbent (Sheng et al., 2010).

3.5 Adsorption Thermodynamics

Thermodynamic parameters of adsorption provide a great deal of information about the type and mechanism of the adsorption process. The Gibbs energy change $\Delta G°$ is calculated through:

$$\Delta G^0 = -RT\ ln\ K \qquad (8a)$$

A negative Gibbs free energy value represents the feasibility and spontaneous nature of the process of adsorption (Din et al., 2014). The distribution constant K can be expressed as;

$$K = C_{ad}/C_e$$

Where C_{ad} (mg/l) and C_e (mg/l) are the concentration of solute adsorbed at equilibrium and the solute concentration in solution at equilibrium respectively while R is the gas constant with a value of 8.314 J mol^{-1} K^{-1}, and T represent the absolute temperature in kelvins. The relationship between ($\Delta G°$) and enthalpy change ($\Delta H°$) and entropy change ($\Delta S°$) of adsorption is expressed as:

$$\Delta G^0 = \Delta H^0 - T\Delta S^0 \qquad (9)$$

Substituting Eq. 8 into Eq. 9;

$$ln\ K = -\Delta H^0/RT + \Delta S^0/R \qquad (10)$$

The values of $\Delta H°$ and $\Delta S°$ are determined from the slope and intercept of the linear plot of ($ln\ K$) versus ($1/T$) represented in **Figure 14A,B** and **Table 1**.

A negative value of Gibb's free energy showed the thermodynamic feasibility and spontaneity of the adsorption process. The positive values of ΔH confirmed the endothermic nature of chromium and lead adsorption Positive values of entropy indicated the increased randomness at the solid-solution interface during the fixation of adsorbate on the active sites of adsorbent. Reddy et al. (2012) applied Moringa oleifera leaves to adsorb Cu^{2+} and noted that $\Delta H^0 = 12.76$ kJ/mol and $\Delta S^0 = 52.6$ J/mole-K, claiming that their adsorption was endothermic. They proposed that the positive entropy change was due to the redistribution of energy between adsorbate and adsorbent (Rafatullah et al., 2012). In applying Aspergillus niger to adsorb $Cu^{2+,}$ Dursun (2006) determined that $\Delta H^0 = 28.9$ kJ/mol and $\Delta S^0 = 168$ J/mole-K. Adsorption in this study was endothermic (Dursun, 2006).

4 CONCLUSION

The present study aimed to use agricultural waste to provide support for the Selenium nanoparticles. The utilization of orange peel was a greener, ecofriendly approach in the synthesis of nanocomposite. Characterization tools confirm the successful synthesis of nanocomposite as witnessed by the clear change in spectra of FTIR and XRD. The batch experiments for the adsorption of metals reveal the successful removal of above 95% for Chromium and Lead. Adsorption capacity was influenced by various factors including pH, temperature and adsorbent dose. Acidic medium was found to be better for the removal of metals. The maximum removal efficiency of 99% was found at the optimum dose and temperature of 20mg and $60°C$ respectively. Furthermore the experimental data was examined with Pseudo-first order, first-order and Pseudo-second order kinetic model, as well as Morris Intraparticle diffusion model where the pseudo second order was best fitted. The adsorption process followed the Langmuir isotherm model verified that OP/Se nanocomposite was found to be favorable for the process of adsorption. The adsorption thermodynamics indicate that adsorption of heavy metals ions is spontaneous ($\Delta G°<0$) and the adsorption increases with increase in temperature so the reaction is endothermic in nature.

DATA AVAILABILITY STATEMENT

The raw data supporting the conclusions of this article will be made available by the authors, without undue reservation.

AUTHOR CONTRIBUTIONS

RA and MA conceived of the idea. MA conducted the experiment. AA, EME, BES and ASK collected the literature review. MTR, AQ and MT provided technical expertise.

MUA. helped in statistical analysis. MTR proofread and provided intellectual guidance. All authors read the first draft, helped in revision, and approved the article. All authors have read and agreed to the published version of the manuscript.

REFERENCES

Ajmal, M., Rao, R. A. K., Ahmad, R., and Ahmad, J. (2000). Adsorption Studies on Citrus Reticulata (Fruit Peel of Orange): Removal and Recovery of Ni(II) from Electroplating Wastewater. *J. Hazard. Mater.* 79, 117–131. doi:10.1016/S0304-3894(00)00234-X

Akbal, F., and Camcı, S. (2011). Copper, Chromium and Nickel Removal from Metal Plating Wastewater by Electrocoagulation. *Desalination* 269, 214–222. doi:10.1016/j.desal.2010.11.001

Akbar, K. F., Hale, W. H., Headley, A. D., and Athar, M. (2006). Heavy Metal Contamination of Roadside Soils of Northern England. *J. Soil & Water Res.* 1, 158–163.

Akinhanmi, T. F., Ofudje, E. A., Adeogun, A. I., Aina, P., and Joseph, I. M. (2020). Orange Peel as Low-Cost Adsorbent in the Elimination of Cd (II) Ion: Kinetics, Isotherm, Thermodynamic and Optimization Evaluations. *Bioresour. Bioprocess.* 7, 1–16. doi:10.1186/s40643-020-00320-y

Al-Ghouti, M. A., Khraisheh, M. A. M., Ahmad, M. N. M., and Allen, S. (2009). Adsorption Behaviour of Methylene Blue onto Jordanian Diatomite: a Kinetic Study. *J. Hazard. Mater.* 165, 589–598. doi:10.1016/j.jhazmat.2008.10.018

Al-Mudhaffar, D. M. H., and Hasan, A. A. A. (2012). Synthesis, Characterization, and Biological Activity of Some New Amino Acid Derivatives Containing Selenium. *Int. J. Appl.* 2. doi:10.1515/revic-2018-0008

Androulaki, E., Barger, A., Bortnikov, V., Cachin, C., Christidis, K., De Caro, A., et al. (2018). "Hyperledger Fabric: a Distributed Operating System for Permissioned Blockchains," in *Proceedings of the Thirteenth EuroSys Conference*, 1–15. doi:10.1145/3190508.3190538

Anhwange, B. A., Ugye, T. J., and Nyiaatagher, T. D. (2009). Chemical Composition of Musa Sapientum (Banana) Peels. *Electron. J. Environ. Agric. Food Chem.* 8, 437–442.

Asfaram, A., Ghaedi, M., Agarwal, S., Tyagi, I., and Kumar Gupta, V. (2015). Removal of Basic Dye Auramine-O by ZnS:Cu Nanoparticles Loaded on Activated Carbon: Optimization of Parameters Using Response Surface Methodology with Central Composite Design. *RSC Adv.* 5, 18438–18450. doi:10.1039/C4RA15637D

Asfaram, A., Ghaedi, M., Hajati, S., Goudarzi, A., and Dil, E. A. (2017). Screening and Optimization of Highly Effective Ultrasound-Assisted Simultaneous Adsorption of Cationic Dyes onto Mn-Doped Fe3O4-Nanoparticle-Loaded Activated Carbon. *Ultrason. Sonochemistry* 34, 1–12. doi:10.1016/j.ultsonch.2016.05.011

Ayatollahi, S. M., Bagheri, Z., and Heydari, S. T. (2013). Agreement Analysis Among Measures of Thinness and Obesity Assessment in Iranian School Children and Adolescents. *Asian J. Sports Med.* 4, 272–280. doi:10.5812/asjsm.34247

Bahig, G., and El-Kadi, A. (2016). "Formal Verification Framework for Automotive UML Designs," in *Proceedings of the 2nd Africa and Middle East Conference on Software Engineering*, 21–27. doi:10.1145/2944165.2944169

Bansode, R. R., Losso, J. N., Marshall, W. E., Rao, R. M., and Portier, R. J. (2003). Adsorption of Volatile Organic Compounds by Pecan Shell- and Almond Shell-Based Granular Activated Carbons. *Bioresour. Technol.* 90, 175–184. doi:10.1016/S0960-8524(03)00117-2

Bathe, K.-J., and Zhang, H. (2004). Finite Element Developments for General Fluid Flows with Structural Interactions. *Int. J. Numer. Meth. Engng.* 60, 213–232. doi:10.1002/nme.959

Bayramoglu, G., and Arica, M. Y. (2018). Adsorption of Congo Red Dye by Native Amine and Carboxyl Modified Biomass of Funalia Trogii: Isotherms, Kinetics and Thermodynamics Mechanisms. *Korean J. Chem. Eng.* 35 (6), 1303–1311. doi:10.1007/s11814-018-0033-9

FUNDING

Begum, K., and Islam, M. (2013). Natural Fibre as a Substitute to Synthetic Fibre in Polymer Composites: a Review. *Res. J. Eng. Sci.* 3, 46–53. View at: Google Scholar.

Belal, A.-A., El-Ramady, H. R., Mohamed, E. S., and Saleh, A. M. (2014). Drought Risk Assessment Using Remote Sensing and GIS Techniques. *Arab. J. Geosci.* 7, 35–53. doi:10.1007/s12517-012-0707-2

Bhatnagar, P., Wickramasinghe, K., Williams, J., Rayner, M., and Townsend, N. (2015). The Epidemiology of Cardiovascular Disease in the UK 2014. *Heart* 101, 1182–1189. doi:10.1136/heartjnl-2015-307516

Biccard, B. M., Madiba, T. E., Kluyts, H. L., Munlemvo, D. M., Madzimbamuto, F. D., Basenero, A., et al. (2018). Perioperative Patient Outcomes in the African Surgical Outcomes Study: a 7-day Prospective Observational Cohort Study. *Lancet* 391, 1589–1598. doi:10.1016/S0140-6736(18)30001-1

Brandstätter, E., Gigerenzer, G., and Hertwig, R. (2008). Risky Choice with Heuristics: Reply to Birnbaum (2008), Johnson, Schulte-Mecklenbeck, and Willemsen (2008), and Rieger and Wang (2008). *Psychol. Rev.* 115 (1), 281–290. doi:10.1037/0033-295X.115.1.281

Buasri, A., Chaiyut, N., Tapang, K., Jaroensin, S., and Panphrom, S. (2012). Equilibrium and Kinetic Studies of Biosorption of Zn(II) Ions from Wastewater Using Modified Corn Cob. *Apcbee Procedia* 3, 60–64. doi:10.1016/j.apcbee.2012.06.046

Cay, S., Uyanik, A., and Ozasik, A. (2004). Single and Binary Component Adsorption of Copper(II) and Cadmium(II) from Aqueous Solutions Using Tea-Industry Waste. *Sep. Purif. Technol.* 38, 273–280. doi:10.1016/j.seppur.2003.12.003

Chukwuemeka-Okorie, H. O., Ekemezie, P. N., Akpomie, K. G., and Olikagu, C. S. (2018). Calcined Corncob-Kaolinite Combo as New Sorbent for Sequestration of Toxic Metal Ions from Polluted Aqua Media and Desorption. *Front. Chem.* 6, 273. doi:10.3389/fchem.2018.00273

Davarnejad, R., and Panahi, P. (2016). Cu (II) Removal from Aqueous Wastewaters by Adsorption on the Modified Henna with Fe 3 O 4 Nanoparticles Using Response Surface Methodology. *Sep. Purif. Technol.* 158, 286–292. doi:10.1016/j.seppur.2015.12.018

Dehghani, M. H., Sanaei, D., Ali, I., and Bhatnagar, A. (2016). Removal of Chromium(VI) from Aqueous Solution Using Treated Waste Newspaper as a Low-Cost Adsorbent: Kinetic Modeling and Isotherm Studies. *J. Mol. Liq.* 215, 671–679. doi:10.1016/j.molliq.2015.12.057

Din, M. I., Hussain, Z., Mirza, M. L., Shah, A. T., and Athar, M. M. (2014). Adsorption Optimization of Lead (II) Using Saccharum Bengalense as a Non-conventional Low Cost Biosorbent: Isotherm and Thermodynamics Modeling. *Int. J. Phytoremediation* 16, 889–908. doi:10.1080/15226514.2013.80302510.1080/15226514.2013.803025

Dobaradaran, S., Nabipour, I., Saeedi, R., Ostovar, A., Khorsand, M., Khajeahmadi, N., et al. (2017). Association of Metals (Cd, Fe, as, Ni, Cu, Zn and Mn) with Cigarette Butts in Northern Part of the Persian Gulf. *Tob. Control* 26, 461–463. doi:10.1136/tobaccocontrol-2016-052931

Dongyan, H. U. A. N. G., Juan, L. I., Ping, J. I. A. N. G., Zhaohui, H. U. A. N. G., Jiahui, S. H. A. O., Mei, S. H. I., .and Jianzhong, Z. H. E. N. G. (2016). Activated Carbon from Biological Sludge Blended with Bituminous Coal: Preparation and its Phenol Adsorption Properties. *Chin. J. Environ. Eng.* 10 (10), 5931–5936.

Doyurum, S., and Çelik, A. (2006). Pb(II) and Cd(II) Removal from Aqueous Solutions by Olive Cake. *J. Hazard. Mater.* 138, 22–28. doi:10.1016/j.jhazmat.2006.03.071

Dursun, A. Y. (2006). A Comparative Study on Determination of the Equilibrium, Kinetic and Thermodynamic Parameters of Biosorption of Copper(II) and Lead(II) Ions onto Pretreated Aspergillus niger. *Biochem. Eng. J.* 28, 187–195. doi:10.1016/j.bej.2005.11.003

Finkelstein, E. A., Graham, W. C. K., and Malhotra, R. (2014). Lifetime Direct Medical Costs of Childhood Obesity. *Pediatrics* 133, 854–862. doi:10.1542/peds.2014-0063

Fu, F., and Wang, Q. (2011). Removal of Heavy Metal Ions from Wastewaters: a Review. *J. Environ. Manag.* 92, 407–418. doi:10.1016/j.jenvman.2010.11.011

Gangadhar, B. H., Sajeesh, K., Venkatesh, J., Baskar, V., Abhinandan, K., Yu, J. W., et al. (2016). Enhanced Tolerance of Transgenic Potato Plants Over-expressing Non-specific Lipid Transfer Protein-1 (StnsLTP1) against Multiple Abiotic Stresses. *Front. Plant Sci.* 7, 1228. doi:10.3389/fpls.2016.01228

Gavrilescu, M. (2014). Removal of Heavy Metals from the Environment by Biosorption. *Eng. Life Sci.* 4, 219–232. doi:10.1002/elsc.200420026

Gupta, D. K., Palma, J. M., and Corpas, F. J. (2016). *Redox State as a Central Regulator of Plant-Cell Stress Responses.* Germany: Springer International Publishing.

Gupta, V. K., Agarwal, S., and Saleh, T. A. (2011). Synthesis and Characterization of Alumina-Coated Carbon Nanotubes and Their Application for Lead Removal. *J. Hazard. Mater.* 185, 17–23. doi:10.1016/j.jhazmat.2010.08.053

Hong, H., Pooladi-Darvish, M., and Bishnoi, P. R. (2003). Analytical Modelling of Gas Production from Hydrates in Porous Media. *J. Can. Petroleum Technol.* 42, 45–56. doi:10.2118/03-11-05

Igwe, J. C., and Abia, A. A. (2007). Adsorption Isotherm Studies of Cd (II), Pb (II) and Zn (II) Ions Bioremediation from Aqueous Solution Using Unmodified and EDTA-Modified Maize Cob. *Eclet. Quím.* 32, 33–42. doi:10.1590/s0100-46702007000100005

Jagadeesh, D., Kanny, K., and Prashantha, K. (2017). A Review on Research and Development of Green Composites from Plant Protein-Based Polymers. *Polym. Compos.* 38, 1504–1518. View at: Publisher Site | Google Scholar. doi:10.1002/pc.23718

Jain, A., Balasubramanian, R., and Srinivasan, M. P. (2016). Hydrothermal Conversion of Biomass Waste to Activated Carbon with High Porosity: A Review. *Chem. Eng. J.* 283, 789–805. doi:10.1016/j.cej.2015.08.014

Jaouali, I., Hamrouni, H., Moussa, N., Nsib, M. F., Centeno, M. A., Bonavita, A., et al. (2018). LaFeO3 Ceramics as Selective Oxygen Sensors at Mild Temperature. *Ceram. Int.* 44, 4183–4189. doi:10.1016/j.ceramint.2017.11.221

Jiang, J., Pi, J., and Cai, J. (2018). The Advancing of Zinc Oxide Nanoparticles for Biomedical Applications. *Bioinorganic Chem. Appl.* doi:10.1155/2018/1062562

Keya, K. N., Kona, A., Kona, N. A., Koly, F. A., Maraz, K. M., Islam, M. N., et al. (2019). Natural Fiber Reinforced Polymer Composites: History, Types, Advantages, and Applications. *Mater Eng. Res.* 1, 69–87. View at: Publisher Site | Google Scholar. doi:10.25082/mer.2019.02.006

Khan, A. S., Yu, S., and Liu, H. (2012). Deformation Induced Anisotropic Responses of Ti-6Al-4V Alloy Part II: A Strain Rate and Temperature Dependent Anisotropic Yield Criterion. *Int. J. Plasticity* 38, 14–26. doi:10.1016/j.ijplas.2012.03.013

Kumar, D., and Gaur, J. P. (2011). Chemical Reaction- and Particle Diffusion-Based Kinetic Modeling of Metal Biosorption by a Phormidium sp.-dominated Cyanobacterial Mat. *Bioresour. Technol.* 102, 633–640. doi:10.1016/j.biortech.2010.08.014

Kumari, S., Badana, A. K., G, M. M., G, S., and Malla, R. (2018). Reactive Oxygen Species: a Key Constituent in Cancer Survival. *Biomark. Insights* 13, 1177271918755391–224. doi:10.1177/1177271918755391

Lai, F. Y., O'Brien, J. W., Thai, P. K., HallChan, W., Chan, G., Bruno, R., et al. (2016). Cocaine, MDMA and Methamphetamine Residues in Wastewater: Consumption Trends (2009-2015) in South East Queensland, Australia. *Sci. Total Environ.* 568, 803–809. doi:10.1016/j.scitotenv.2016.05.181

Landaburu-Aguirre, J., Pongrácz, E., Perämäki, P., and Keiski, R. L. (2010). Micellar-enhanced Ultrafiltration for the Removal of Cadmium and Zinc: Use of Response Surface Methodology to Improve Understanding of Process Performance and Optimisation. *J. Hazard. Mater.* 180, 524–534. doi:10.1016/j.jhazmat.2010.04.066

Lau, S. K., Boutros, P. C., Pintilie, M., Blackhall, F. H., Zhu, C.-Q., Strumpf, D., et al. (2007). Three-Gene Prognostic Classifier for Early-Stage Non-small-cell Lung Cancer. *Jco* 25, 5562–5569. doi:10.1200/jco.2007.12.0352

Le Quéré, C., Moriarty, R., Andrew, R. M., Canadell, J. G., Sitch, S., Korsbakken, J. I., et al. (2015). Global Carbon Budget 2015. *Earth Syst. Sci. Data* 7, 349–396. doi:10.5194/essd-7-349-2015

Lenz, G., Wright, G. W., Emre, N. C. T., Kohlhammer, H., Dave, S. S., Davis, R. E., et al. (2008). Molecular Subtypes of Diffuse Large B-Cell Lymphoma Arise by Distinct Genetic Pathways. *Proc. Natl. Acad. Sci. U.S.A.* 105, 13520–13525. doi:10.1073/pnas.0804295105

Lertlapwasin, R., Bhawawet, N., Imyim, A., and Fuangswasdi, S. (2010). Ionic Liquid Extraction of Heavy Metal Ions by 2-aminothiophenol in 1-Butyl-3-Methylimidazolium Hexafluorophosphate and Their Association Constants. *Sep. Purif. Technol.* 72, 70–76. doi:10.1016/j.seppur.2010.01.004

Li, S., Tan, H.-Y., Wang, N., Zhang, Z.-J., Lao, L., Wong, C.-W., et al. (2015). The Role of Oxidative Stress and Antioxidants in Liver Diseases. *Ijms* 16, 26087–26124. doi:10.3390/ijms161125942

Libert, S., Zwiener, J., Chu, X., VanVoorhies, W., Roman, G., and Pletcher, S. D. (2007). Regulation of Drosophila Life Span by Olfaction and Food-Derived Odors. *Science* 315, 1133–1137. doi:10.1126/science.1136610

Liu, Y., Lim, J., and Teoh, S.-H. (2013). Review: Development of Clinically Relevant Scaffolds for Vascularised Bone Tissue Engineering. *Biotechnol. Adv.* 31, 688–705. doi:10.1016/j.biotechadv.2012.10.003

Luisa, P., Lopes, C., Macena, M., Esteves, B., and Raquel, P. F. (2021). Ideal pH for the Adsorption of Metal Ions Cr^{6+}, Ni^{2+}, Pb^{2+} in Aqueous Solution with Different Adsorbent Materials. *Open Agric.* 6, 115–123. doi:10.1515/opag-2021-0225

Mangal, A., Kumar, V., Panesar, S., Talwar, R., Raut, D., and Singh, S. (2015). Updated BG Prasad Socioeconomic Classification, 2014: A Commentary. *Indian J. Public Health* 59, 42. doi:10.4103/0019-557X.152859

Mehmoud, A. M., and Halwany, M. M. (2014). Adsorption of Cadmium onto Orange Peels: Isotherms, Kinetics and Thermodynamics. *J. Chromatogr.* 5, 5. doi:10.4172/2157-7064.1000238

Mohammed, L., Ansari, M. N., Pua, G., Jawaid, M., and Islam, M. S. (2015). A Review on Natural Fibre Reinforced Polymer Composite and its Applications. *Int. J. Polym. Sci.* 2015. Article ID 243947, View at: Google Scholar. doi:10.1155/2015/243947

Nie, W., Tsai, H., Asadpour, R., Blancon, J.-C., Neukirch, A. J., Gupta, G., et al. (2015). High-efficiency Solution-Processed Perovskite Solar Cells with Millimeter-Scale Grains. *Science* 347, 522–525. doi:10.1126/science.aaa0472

Nriagu, J. O. (1996). A History of Global Metal Pollution. *Science* 272, 223. doi:10.1126/science.272.5259.223

Nuhoglu, Y., and Oguz, E. (2003). Removal of Copper(II) from Aqueous Solutions by Biosorption on the Cone Biomass of Thuja Orientalis. *Process Biochem.* 38 (11), 1627–1631. doi:10.1016/S0032-9592(03)00055-4

Ofomaja, A. E., Naidoo, E. B., and Pholosi, A. (2020). Intraparticle Diffusion of Cr (VI) through Biomass and Magnetite Coated Biomass: A Comparative Kinetic and Diffusion Study. *South Afr. J. Chem. Eng.* 32 (1), 39–55.

Ofudje, E. A., Rajendran, A., Adeogun, A. I., Idowu, M. A., Kareem, S. O., and Pattanayak, D. K. (2018). Synthesis of Organic Derived Hydroxyapatite Scaffold from Pig Bone Waste for Tissue Engineering Applications. *Adv. Powder Technol.* 29, 1–8. doi:10.1016/j.apt.2017.09.008

Ozalp, V. C., Bayramoglu, G., Erdem, Z., and Arica, M. Y. (2015). Pathogen Detection in Complex Samples by Quartz Crystal Microbalance Sensor Coupled to Aptamer Functionalized Core-Shell Type Magnetic Separation. *Anal. Chim. Acta* 853, 533–540. doi:10.1016/j.aca.2014.10.010

Rafatullah, M., Sulaiman, O., Hashim, R., and Ahmad, A. (2012). Removal of Cadmium (II) from Aqueous Solutions by Adsorption Using Meranti Wood. *Wood Sci. Technol.* 46, 221–241. doi:10.1007/s00226-010-0374-y

Rajoriya, S., and Kaur, B. (2014). Adsorptive Removal of Zinc from Waste Water by Natural Biosorbents. *Int. J. Eng. Sci. Invent.* 3, 60–80.

Rangabhashiyam, S., Nakkeeran, E., Anu, N., and Selvaraju, N. (2015). Biosorption Potential of a Novel Powder, Prepared from Ficus Auriculata Leaves, for Sequestration of Hexavalent Chromium from Aqueous Solutions. *Res. Chem. Intermed.* 41, 8405–8424. doi:10.1007/s11164-014-1900-6

Rani, K. P., and Ravindhranath, K. (2014). Removal of Ammonia from Polluted Waters Using New Bio-Sorbents. *J. Chem. Pharm. Res.* 6, 889–900.

Robati, D., Mirza, B., Rajabi, M., Moradi, O., Tyagi, I., Agarwal, S., et al. (2016). Removal of Hazardous Dyes-BR 12 and Methyl Orange Using Graphene Oxide as an Adsorbent from Aqueous Phase. *Chem. Eng. J.* 284, 687–697. doi:10.1016/j.cej.2015.08.131

Sahu, P., and Gupta, M. (2020). A Review on the Properties of Natural Fibres and its Bio-Composites: Effect of Alkali Treatment. *Proc. Institution Mech. Eng. Part L J. Mater. Des. Appl.* 234, 198–217. View at: Google Scholar. doi:10.1177/1464420719875163

Sahu, P., and Gupta, M. K. (2019). Lowering in Water Absorption Capacity and Mechanical Degradation of Sisal Composites by Effect of Eco-Friendly Treatment and Coating. *Polym. Compos.* 41, 668–681. doi:10.1002/pc.25397

Shaker, K., Umair, M., Shahid, S., Jabbar, M., Ullah Khan, R. M. W., Zeeshan, M., et al. (2020). Cellulosic Fillers Extracted from Argyreia Speciose Waste: a Potential Reinforcement for Composites to Enhance Properties. *J. Nat. Fibers*, 1–13. View at: Publisher Site | Google Scholar. doi:10.1080/15440478.2020.1856271

Sharma, K., Kaith, B. S., Kumar, V., Kalia, S., Kumar, V., and Swart, H. C. (2014). Water Retention and Dye Adsorption Behavior of Gg-Cl-Poly(acrylic Acid-Aniline) Based Conductive Hydrogels. *Geoderma* 232-234, 45–55. doi:10.1016/j.geoderma.2014.04.035

Sheng, G. D., Shao, D. D., Ren, X. M., Wang, X. Q., Li, J. X., Chen, Y. X., et al. (2010). Kinetics and Thermodynamics of Adsorption of Ionizable Aromatic Compounds from Aqueous Solutions by As-Prepared and Oxidized Multiwalled Carbon Nanotubes. *J. Hazard. Mater.* 178, 505–516. doi:10.1016/j.jhazmat.2010.01.110

Shoukry, Y., El-Kharashi, M. W., Hammad, S., Kumar, A., and Bahig, G. (2015). "Software Allocation in Automotive Networked Embedded Systems: A Graph-Based Approach," in *Languages, Design Methods, and Tools for Electronic System Design*, 207–221. doi:10.1007/978-3-319-06317-1_11

Song, L. X., Yang, Z. K., Teng, y., Xia, J., and Du, P. (2013). Nickle Oxide Nanoflowers: Formation, Structure, Magnetic Property and Adsorptive Performance towards Organic Dyes and Heavy Metal Ions. *J. Mater. Chem. A* 1, 18731–8736. doi:10.1039/c3ta12114c

Srivastava, N., and Banik, B. K. (2003). Bismuth Nitrate-Catalyzed Versatile Michael Reactions. *J. Org. Chem.* 68, 2109–2114. doi:10.1021/jo026550s

Sulyman, A. I., Alwarafy, A., MacCartney, G. R., Rappaport, T. S., and Alsanie, A. (2016). Directional Radio Propagation Path Loss Models for Millimeter-Wave Wireless Networks in the 28-, 60-, and 73-GHz Bands. *IEEE Trans. Wirel. Commun.* 15, 6939–6947. doi:10.1109/twc.2016.2594067

Tan, I. A. W., Ahmad, A. L., and Hameed, B. H. (2008). Adsorption of Basic Dye on High-Surface-Area Activated Carbon Prepared from Coconut Husk: Equilibrium, Kinetic and Thermodynamic Studies. *J. Hazard. Mater.* 154, 337–346. doi:10.1016/j.jhazmat.2007.10.031

Tee, K. P., Ge, S. S., and Tay, E. H. (2009). Barrier Lyapunov Functions for the Control of Output-Constrained Nonlinear Systems. *Automatica* 45, 918–927. doi:10.1016/j.automatica.2008.11.017

Thyavihalli Girijappa, Y. G., Mavinkere Rangappa, S., Parameswaranpillai, J., and Siengchin, S. (2019). Natural Fibers as Sustainable and Renewable Resource for Development of Eco-Friendly Composites: a Comprehensive Review. *Front. Mater.* 6. View at: Publisher Site | Google Scholar. doi:10.3389/fmats.2019.00226

Ugbolue, S. C., Kim, Y. K., Warner, S. B., Fan, Q., Yang, C. L., Kyzymchuk, O., et al. (2011). The Formation and Performance of Auxetic Textiles. Part II: Geometry and Structural Properties. *J. Text. Inst.* 102, 424–433. doi:10.1080/00405000.2010.486183

Updyke, K. M., Nguyen, T. B., and Nizkorodov, S. A. (2012). Formation of Brown Carbon via Reactions of Ammonia with Secondary Organic Aerosols from Biogenic and Anthropogenic Precursors. *Atmos. Environ.* 63, 22–31. doi:10.1016/j.atmosenv.2012.09.012

Verma, S., and Singh, S. (2008). Current and Future Status of Herbal Medicines. *Vet. World* 2, 347. doi:10.5455/vetworld.2008.347-350

Wang, J., Agrawala, M., and Cohen, M. F. (2007). "Soft Scissors: an Interactive Tool for Realtime High Quality Matting," in *ACM SIGGRAPH Papers*. doi:10.1145/1275808.1276389

Wannahari, R., Sannasi, P., Nordin, M. F., and Mukhtar, H. (2018). Sugarcane Bagasse Derived Nano Magnetic Adsorbent Composite (SCB-NMAC) for Removal of Cu2+ from Aqueous Solution. *ARPN J. Eng. Appl. Sci.* 13, 1–9.

Weber, W. J., Jr, and Morris, J. C. (1963). Kinetics of Adsorption on Carbon from Solution. *J. Sanit. Engrg. Div.* 89, 31–59. doi:10.1061/jsedai.0000430

Yobas, L., Feng Cheow, L., Tang, K.-C., Yong, S.-E., Kye-Zheng Ong, E., Wong, L., et al. (2009). A Self-Contained Fully-Enclosed Microfluidic Cartridge for Lab on a Chip. *Biomed. Microdevices* 11, 1279–1288. doi:10.1007/s10544-009-9347-z

Zeeshan, M., Ali, M., Anjum, A. S., and Nawab, Y. (2021). Optimization of Mechanical/thermal Properties of Glass/flax/waste Cotton Hybrid Composite. *J. Industrial Text.* 51, 768–787. doi:10.1177/1528083719891420

Zhang, L., Dawes, W. R., and Walker, G. R. (2011). Response of Mean Annual Evapotranspiration to Vegetation Changes at Catchment Scale. *Water Resour. Res.* 37, 701–708. doi:10.1029/2000WR900325

Zhang, Y., Tan, Y.-W., Stormer, H. L., and Kim, P. (2005). Experimental Observation of the Quantum Hall Effect and Berry's Phase in Graphene. *Nature* 438, 201–204. doi:10.1038/nature04235

Zheng, Z., XiaAmbinakudige, H., Ambinakudige, S., Qin, Y., Li, Y., Xie, Z., et al. (2019). Spatial Accessibility to Hospitals Based on Web Mapping API: An Empirical Study in Kaifeng, China. *Sustainability* 11, 1160. doi:10.3390/su11041160